

1 *Conference Proceedings Paper*

2 **Earthquake Damage Assessment Based on Deep** 3 **Learning Method Using VHR Images**

4 **Masoud Moradi**¹, **Reza Shah-Hosseini**^{2,*}

5 ¹ School of Surveying and Geospatial Engineering, College of Engineering, University of Tehran, Iran;
6 masoudmoradi@ut.ac.ir

7 ² School of Surveying and Geospatial Engineering, College of Engineering, University of Tehran, Iran;
8 rshahosseini@ut.ac.ir

9 * Correspondence: rshahosseini@ut.ac.ir; Tel.: +98-21-6111-4527

10 **Abstract:** One of the numerous fundamental tasks to perform rescue operations after the
11 earthquake, check the status of buildings that have been destroyed. The methods to obtain the
12 damage map are two categories Shared. The first group of methods uses data before and after the
13 earthquake, and the second group only uses the data after the earthquakes that we want to offer a
14 flexible and according to information that we are available to achieve the damage map. In this paper,
15 we work on VHR satellite images of Haiti, and UNet which is a convolution network. The learning
16 algorithms profound changes to improve the results were intended to identify the damage of the
17 buildings caused by the earthquake. The deep learning algorithms require very training data that
18 it's one of the problems that we want to solve. As well as Unlike previous studies by examining
19 pixel by pixel degradation, ultimate precision to increase that shows the success of this approach
20 felt and has been able to reach the overall accuracy of 68.71%. The proposed method for other
21 natural disasters such as rockets, explosions, tsunamis, and floods also destroyed buildings in urban
22 areas is to be used.

23 **Keywords:** Damage detecton, Deep Learning, UNet, VHR Satellite Images, Earthquake.
24

25 **1. Introduction**

26 The world has constantly influenced natural disasters such as earthquakes, floods, and tsunami
27 during civilization. They are considered to be extremely tragic threats and ruined for human security
28 and property. A quick evaluation of infrastructure damage after a dangerous event has an essential
29 role in emergency response management and recovery planning [1,2].

30 The traditional approach to estimating the spatial distribution of earthquake losses in buildings
31 through building field inspection is made by a volunteer group consisting of engineers, architects,
32 and other construction industry professionals. This precise inspection process is essential because
33 evaluations are reliable and give us valuable information on the damaged building's seismic function.
34 However, the duration of these inspections makes them impossible for emergency support and
35 planning for early recovery. Depending on the availability of qualified specialists and the
36 geographical distribution of damaged buildings, the field inspection process can last for months [3].

37 Therefore, for decades, remote sensing techniques play an essential role in examining the
38 earthquake's data damage, especially due to its fast availability after catastrophic and large coverage.
39 In most studies, remote sensing measurements have been used to detect collapsed buildings using
40 different methods before and after the event. Some researchers have only used post-event

41 information and the similarity between damaged buildings that use it to distinguish between
42 destroyed and undamaged buildings that limit this method's accuracy [4,6].

43 As the main sources of remote sensing, optical images usually provide only two-dimensional
44 information that is not suitable for detecting objects; using LIDAR and SAR can improve
45 determination and identification, especially for three-dimensional objects. Because information about
46 The height, especially for the three-dimensional interpretation of the building's state, can be detected
47 by damaged and collapsed buildings by comparing the altitude information before and after the
48 event in urban areas. The method of producing accurate altitude data is tough and expensive, which
49 leads to the inaccessibility of the precise 3D data before and after the earthquake. UAV allows for
50 higher resolution images and cloud 3D points. But, the preparation of UAV images is challenging
51 before the earthquake because UAV images are not continually covering all regions of the world.
52 However, satellite images are still the primary and commonest source for damage assessment. For
53 this reason, they are more reliable and more accessible to detect the destruction of buildings [7-9].

54 With the rapid improvement of satellite optics sensors' spatial resolution, Optical data is
55 promising data for identifying earthquake damages. However, achieving remote sensing VHR
56 images before the earthquake is not easy. Therefore, in new studies, We have tried to achieve good
57 results without having the before event information. This has led to valuable algorithms that can use
58 with both access and not access to data before the earthquake. The other problem with satellite images
59 is that they can't detect damage to the building's length due to the imaging of the above [10,11].

60 The most common method is to detect damage based on change detection techniques. Images
61 before and after an event have been collected and create an image difference, representing the
62 difference between the two datasets. However, this method limits the requirement to have two sets
63 of before and after the earthquake that may not always be available. In such circumstances, machine
64 learning methods had been introduced. Deep learning, one of the advanced techniques in the field of
65 machine learning as the best method for complex and non-linear feature extraction, is at a high level.
66 In recent years, convolutional neural networks (CNN) due to outstanding performance in extracting
67 features on remote sensing have been widely used [12,13].

68 In terms of operational response to the disaster, many challenges remain, two of them to declare
69 that we have and try to solve these challenges [14].

70
71 1. Good performance of deep learning algorithms is limited to the size of data available, and the
72 network structure is considered. One of the most critical challenges for using a deep learning method
73 for monitoring the buildings damaged in the disaster is that the training images of damaged targets
74 are usually not very much. In terms of operational response to the disaster, many challenges remain,
75 two of them to declare that we have and try to solve these challenges.

76
77 2. The size of blocks that have been labeled as undamaged or damaged buildings by the algorithm
78 is ultimately a significant impact on overall accuracy. Previous studies major ways only a label on a
79 large block was allocated. However, this block contains a large number of pixels is irrelevant.
80 Therefore, theoretically, the pixel-based labeling method is more accurate [15,16].

81

U-Net, which is essentially a convolution network, can ultimately reduce the challenges, and we change its layers to make it better performance [17].

In this study, the convolution neural network U-net for Monitoring Haiti earthquake damage on pixel-based images with high-resolution remote sensing is implemented.

2. Experiments

2.1. Datasets

On January 12th, 2010, an earthquake with a magnitude of 7 on the Richter scale hit Port-au-Prince, capital of Haiti, scrambled. In Port-au-Prince and in the southern areas of Haiti, about 97,294 houses completely destroyed and 188,383 houses have suffered damage [18]. The study area is part of the city of Port-au-Prince is shown in Figure 1. In this study, by Worldview 2 satellite imagery, pre-image acquired on January 16th, 2010, and post-image obtained on October 1st, 2009. The satellite image consists of four multi-spectral bands with a resolution of 2 m and one high-resolution panchromatic band with 0.5 m resolution. Four high-resolution colored bands are used in this algorithm, through integrating the multi-spectral and panchromatic bands. To assess damaged and undamaged buildings use the International Institute UNITAR / UNOSAT data and Earthquake Geospatial Data Dataverse (CGA, Harvard Univ) dataset with visual interpretation [19,20].



Figure 1. The location of the study area

View of the area before and after the earthquake is shown in Figure 2.



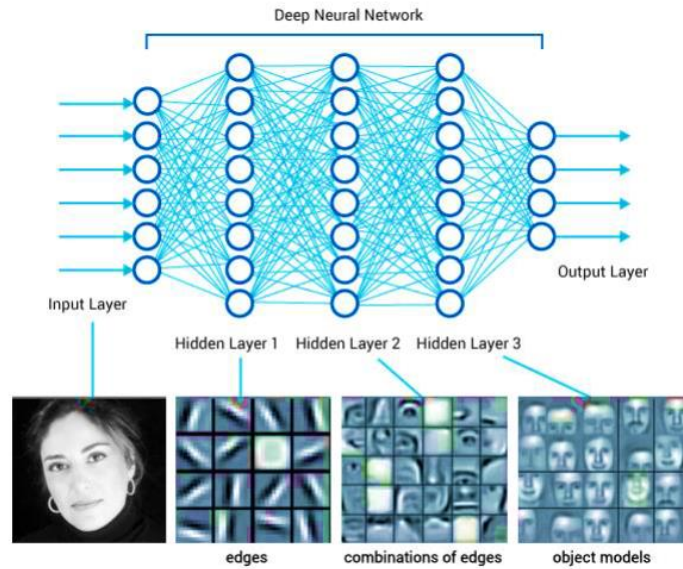
Figure 2. The right image is before the earthquake, and the left image is after the earthquake.

2.2. Method

In this study, an approach based on deep learning algorithms and neural networks for monitoring the buildings destroyed by the earthquake is presented. In the way that we're going to

109 explain it, based on previous studies on the use of VHR optical data is emphasized. The solution
 110 proposed to lack of access to the data before the earthquake [21-23].

111 Deep learning is said a neural network with a large number of hidden layers to extract many
 112 features from raw data. Data can be an image, pixel, signal, and so on. The different architecture of
 113 this kind exists today. The number of layers greater (deeper), so the more non-linear characteristics
 114 are obtained which is why we are interested in deep learning. Figure 3 shows the general view of the
 115 deep learning networks. Unlike deep learning, machine learning extracts features by itself, and they
 116 need to identify the characteristics and feature engineering [24-26].



117

118 **Figure 3.** Design of layers of the deep learning network

119 The UNet algorithm, due to high precision, high-speed processing, and learning, no need for
 120 large data sets to learn and complex and expensive hardware, in recent years Popular in detection
 121 the objects of the image and image processing has become. The characteristics of this network enable
 122 us to overcome two major challenges that we mentioned in the introduction [27,28].

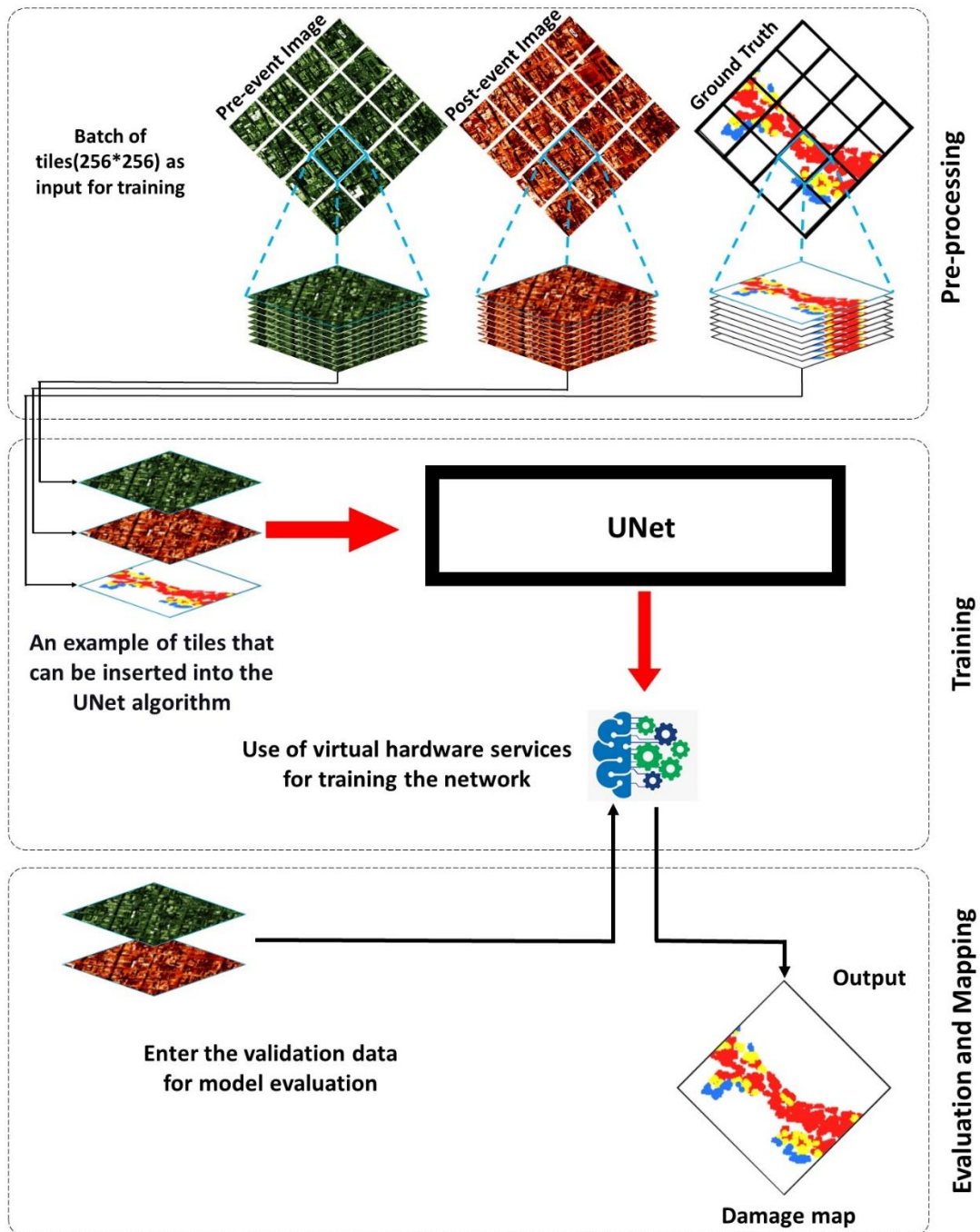


Figure 4. The framework proposed in this paper for monitoring the destruction of buildings in earthquake

۱۲۳
۱۲۴
۱۲۵
۱۲۶

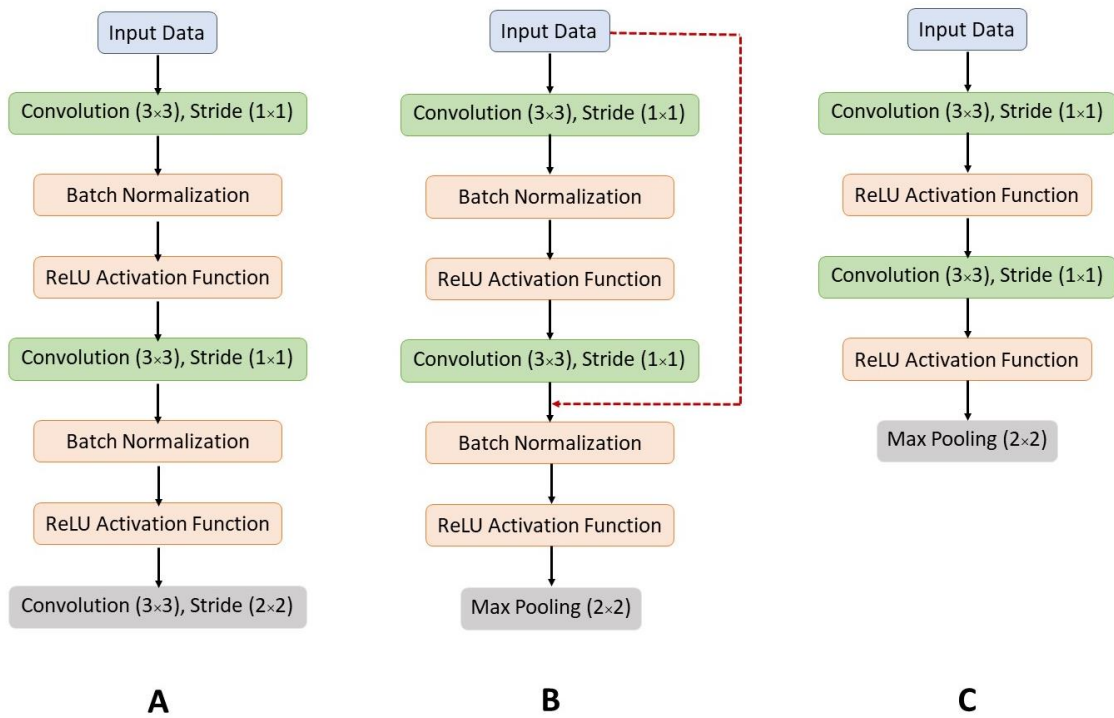
۱۲۷ 2.2.1. Pre-processing

۱۲۸ The images collected before and after the event were compiled into a large image. The co-
 ۱۲۹ registration procedure was implemented on the pre and post-event images. Bands of pre-post images
 ۱۳۰ pan sharpened and stacked together [29]. At this stage, each pixel should be assigned a value of zero or
 ۱۳۱ one that reflects the state of the destruction of the building. Both images and ground-truth data of
 ۱۳۲ building damage were projected into the UTM/WGS84 geo-referenced coordinate system.
 ۱۳۳ Theoretically and ideally, the image tiles with the pixel size of an arbitrary 2^n are suitably used as the

134 input [30]. When selecting random patches to do the training, we try to choose the patches that more
 135 than half of the pixels within them labeled as undamaged or damaged, it is.
 136

137 2.2.2. Network Architecture and training

138 U-net originated from Ronneberger in 2015 [31]. The blocks of neural network units of U-net, U-
 139 net adopted in this study, and Deep Residual U-net that proposed by Zhang in 2018 are shown in
 140 Figure 5 [31-33].



141
 142 **Figure 5.** Blocks of neural network units. (a) Neural unit of U-net in this work. (b) Neural unit in Deep
 143 Residual U-net. (c) Neural unit in general U-net.
 144

145 It has already been shown in many studies that normalizing input data on different architectures
 146 to accelerate network convergence. The use of the Batch Normalization in deep learning algorithms
 147 makes sustainable education and training operations faster network [34]. So Residual U-net network,
 148 as well as our proposed network of Batch Normalization, is used. We normalize the input layer by
 149 adjusting and scaling the activations. for instance , once we have features from 0 to 1 and a few from
 150 1 to 1000, we should always normalize them to hurry up learning. If the input layer is taking
 151 advantage of it, why not do an equivalent thing also for the values within the hidden layers, that are
 152 changing all the time, and get 10 times or more improvement in the training speed [35,36].

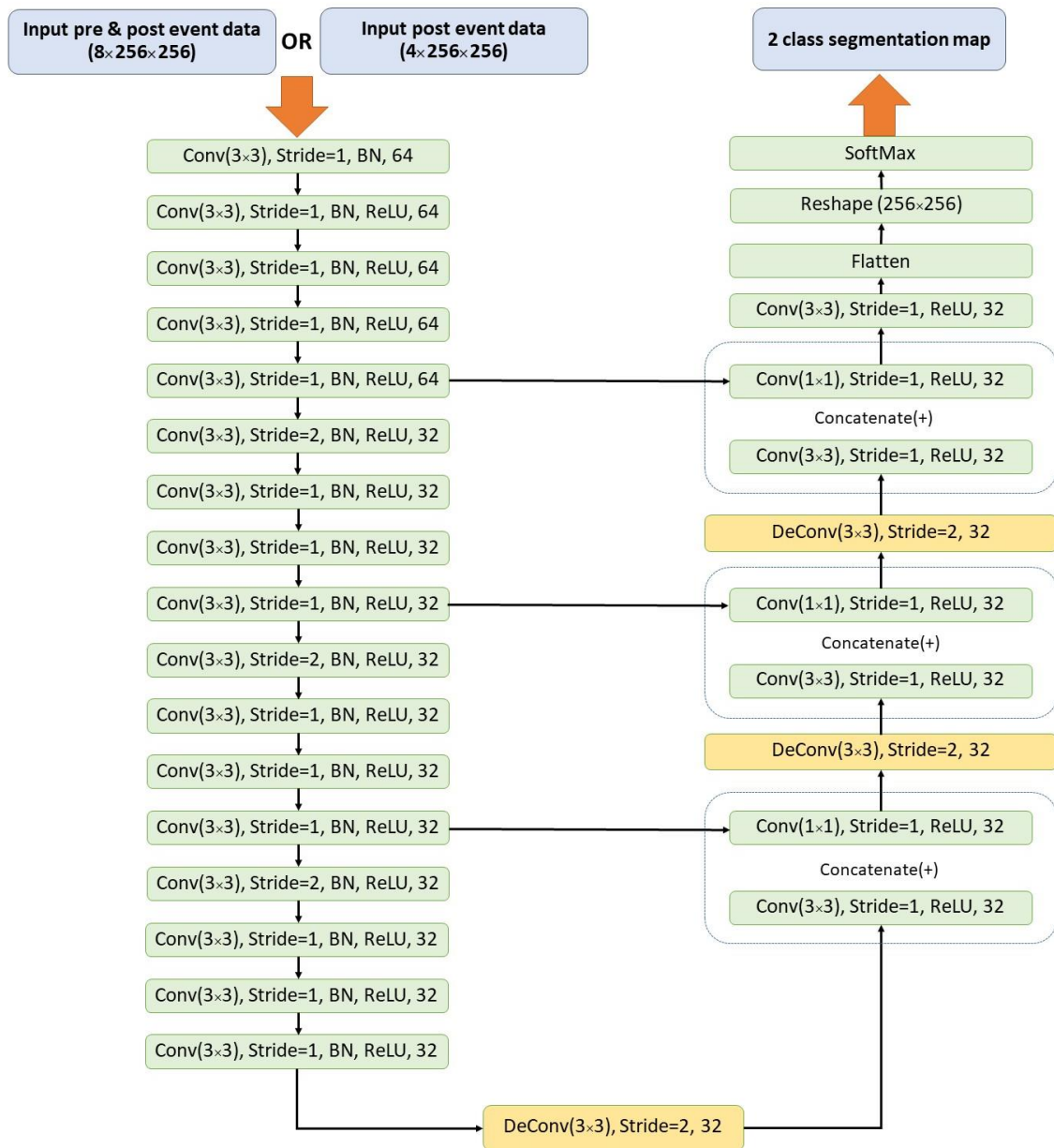


Figure 6. Architecture of the U-net in this study

103

104

100

106 The max-pooling layer used in general U-net was replaced by a convolutional layer with a stride of
 107 2 because the convolutional layer with increased stride outperforms the max-pooling with regards
 108 to several image recognition benchmarks as shown in Figure 5 [37].

109 To reduce the calculation time cost, we decreased the filter number to 50% of the first. This strategy
 110 was recommended in many studies because it was shown useful for remote-sensing recognition
 111 tasks [38].

112 We use a batch size of 25 and a patch size of 256×256 pixels for the Unet models. The models were
 113 trained for 50 epochs. We trained the network with a learning rate of 0.01 for all epochs. RMSProb
 114 is used for parameter optimization that is suitable for large datasets. The employed loss function is
 115 cross-entropy.

166 2.2.3. Development Environment

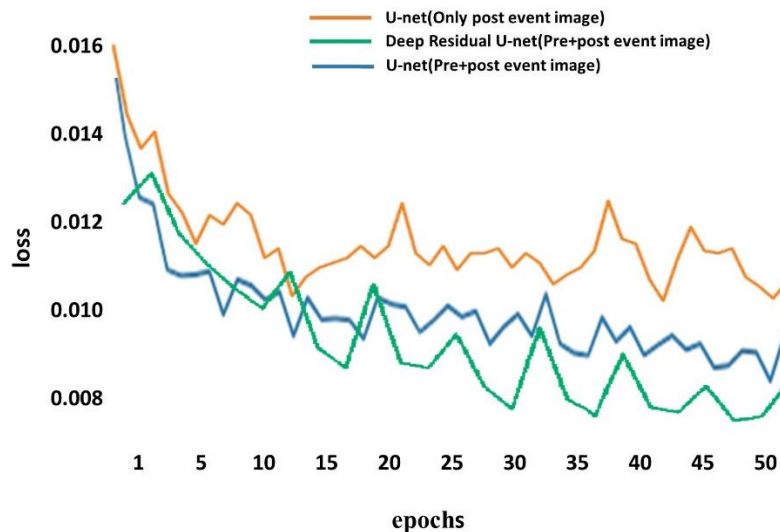
167 In this work, we used the Deep Learning Studio (DLS) and Peltarion as the deep learning
 168 framework [39,40]. DLS is DeepCognition’s web-based software, that designs networks and trains
 169 deep learning algorithms for Windows and Linux. DLS supports deep learning networks for image
 170 recognition tasks. All experimentation and modeling environment tasks are implemented in Deep
 171 Learning Studio Virtual Machine (DLSVM).

172 The virtual machine is configured with 32 GB of RAM, a 2.30 GHz 2-core Intel(R) Xeon(R) CPU,
 173 and a 1.59 GHz NVIDIA Tesla T4 GPU 16GB DDR6 with 50 GB memory [39,40].

174 The data are preprocessed and analyzed in Python using the GDAL, NumPy, pandas, OpenCV,
 175 Scipy, Scikit-image, Scikit-learn, Pillow, MKL, and Tiff file libraries. The deep learning algorithms are
 176 achieved in the Deep Learning Studio (DLS) which is a robust GUI, partially free, and easy-to-use
 177 framework. It can be used in the cloud or on our infrastructure.

178 **3. Results**

179 In this study, we completed 50 epochs for both the U-net model and deep residual U-net to get
 180 the trained building damage recognition model [31,32]. The relation between the cross-entropy loss
 181 and the iteration of epochs is shown in Figure 5. Trend graphs in Figure 7 show that our proposed
 182 method considerably noticeably improves results. Both networks till epoch 15 are close to each other,
 183 and not much difference between them.



184 **Figure 7.** Relation between the loss and the number of epochs during the training.
 185

186 Here, the U-net has a much lower omission error (28.1% undamaged, and 39.3% damaged) than
 187 the deep residual U-net (37.7% undamaged, and 47.2% damaged). The overall accuracy of our
 188 proposed approach 69.71 and the overall accuracy of deep residual U-net 62.5%, which is shown the
 189 method is proposed in this paper proves the performance of the network. The Kappa value for U-net
 190 in this paper is 37.7%.

191 Some buildings were classified incorrectly, because of the orthographic projection characteristic of
 192 the optical remote sensing measurement, the sensor can only record the information on top of each
 193 object, and the damage situation under the roof is not reflected. An example is shown in figure 8
 194 [41,42].



195

196

197

198

199

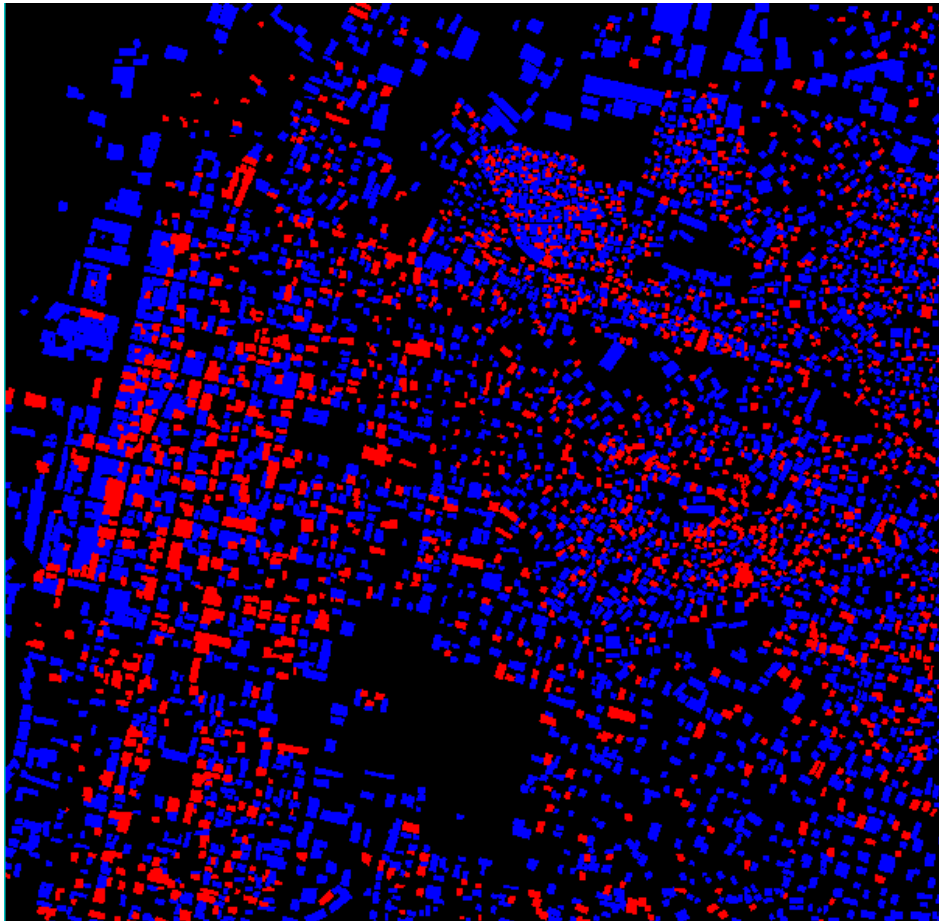
Figure 8. An example of collapsed buildings in the earthquake which incorrectly classified. The image doesn't relate to Haiti earthquake.

200

201

202

The final result of the buildings damage map shown in Figure 9. Although the number of buildings damaged and safe is almost equal, but about three times the pixels dedicated to undamaged building more than buildings have been destroyed. The black area relates to parks, slums, and tents survivors as well as other items that are not within the building kind.



203

204

205

206

207

Figure 9. Final damage Map- The blue colour represents safe buildings, and the red colour represents damaged buildings.

From the availability of data to achieve the final map takes less than 7 hours that very faster than the field inspection and this advantage of this approach.

208 4. Discussion

209 This model was demonstrated for mapping the earthquake damage, but the framework also
210 works for other hazards such as floods, missile attacks, hurricanes, and many natural and unnatural
211 disasters. To generalize this framework to other tragic event types, the VHR satellite image and
212 corresponding reference data for different disaster types should be used to training the new model.
213 The proposed model is a supervised classification model. It can be simply implemented to react to
214 future hazards after these models are well developed.

215 The role of building footmark data is to create training data labels. It is considering that the label
216 of land covers the jungle, water, etc. The non-built-up regions are also available, and we can train a
217 new model that does not depend on the building footprint data. From this aspect, the proposed
218 framework does not depend on building footprint data and is a generalized framework.

219 5. Conclusions

220 Dominance image processing and artificial intelligence in the field of images of remote sensing,
221 especially with the development of algorithms for deep learning, continually grow, but unlike other
222 issues that improved very significantly, but in remote sensing a little performance increased, so still,
223 need to research and further studies of the potential of the computer world in the field of geographical
224 sciences and image processing used.

225 **Acknowledgments:** We would like to thank Deep Cognition for providing the Deep Learning Studio (DLS)
226 service and Peltarion that is a cloud-based operational AI platform that allows you to build and deploy your
227 deep learning models. The service offers an end-to-end platform that lets you do everything from pre-processing
228 your data to building models and putting them into production. All of this runs in the cloud and developers get
229 access to a graphical user interface for building and testing their models. We would also like to show our great
230 gratitude to the International Institute UNITAR / UNOSAT for providing the reference data.

231 **Author Contributions:** M.M. conceived and designed the experiments; M.M. performed the experiments; M.M.
232 and R.S. analyzed the data; R.S. contributed materials and analysis tools; M.M and R.S. wrote the paper.

233 **Conflicts of Interest:** The authors declare no conflict of interest.

234 Abbreviations

235 The following abbreviations are used in this manuscript:

236 References

- 237 1. Anniballe, R.; Noto, F.; Scalia, T.; Bignami, C.; Stramondo, S.; Chini, M.; Pierdicca, N. Earthquake damage
238 mapping: An overall assessment of ground surveys and VHR image change detection after L'Aquila 2009
239 earthquake. *Remote sensing of environment* **2018**, *210*, 166-178.
- 240 2. Bialas, J.; Oommen, T.; Rebbapragada, U.; Levin, E. Object-based classification of earthquake damage from
241 high-resolution optical imagery using machine learning. *Journal of Applied Remote Sensing* **2016**, *10*, 036025.
- 242 3. Dong, L.; Shan, J. A comprehensive review of earthquake-induced building damage detection with remote
243 sensing techniques. *ISPRS Journal of Photogrammetry and Remote Sensing* **2013**, *84*, 85-99.
- 244 4. Cooner, A.J.; Shao, Y.; Campbell, J.B. Detection of Urban Damage Using Remote Sensing and Machine
245 Learning Algorithms: Revisiting the 2010 Haiti Earthquake. *Remote Sensing* **2016**, *8*, doi:10.3390/rs8100868.
- 246 5. Gokon, H.; Koshimura, S. Mapping of building damage of the 2011 Tohoku earthquake tsunami in Miyagi
247 Prefecture. *Coastal Engineering Journal* **2012**, *54*, 1250006.
- 248 6. Menderes, A.; Erenen, A.; Sarp, G. Automatic Detection of Damaged Buildings after Earthquake Hazard by
249 Using Remote Sensing and Information Technologies. *Procedia Earth and Planetary Science* **2015**, *15*, 257-262,
250 doi:https://doi.org/10.1016/j.proeps.2015.08.063.
- 251 7. Novikov, G.; Trekin, A.; Potapov, G.; Ignatiev, V.; Burnaev, E. Satellite imagery analysis for operational
252 damage assessment in emergency situations. In Proceedings of International Conference on Business
253 Information Systems; pp. 347-358.

- 204 8. Taskin Kaya, G.; Musaoglu, N.; Ersoy, O.K. Damage assessment of 2010 Haiti earthquake with post-
 205 earthquake satellite image by support vector selection and adaptation. *Photogrammetric Engineering &*
 206 *Remote Sensing* **2011**, *77*, 1025-1035.
- 207 9. Tong, X.; Hong, Z.; Liu, S.; Zhang, X.; Xie, H.; Li, Z.; Yang, S.; Wang, W.; Bao, F. Building-damage detection
 208 using pre- and post-seismic high-resolution satellite stereo imagery: A case study of the May 2008
 209 Wenchuan earthquake. *ISPRS Journal of Photogrammetry and Remote Sensing* **2012**, *68*, 13-27,
 210 doi:<https://doi.org/10.1016/j.isprsjprs.2011.12.004>.
- 211 10. Voigt, S.; Schneiderhan, T.; Twele, A.; Gähler, M.; Stein, E.; Mehl, H. Rapid damage assessment and
 212 situation mapping: learning from the 2010 Haiti earthquake. *Photogrammetric Engineering and Remote*
 213 *Sensing (PE&RS)* **2011**, *77*, 923-931.
- 214 11. Duarte, D.; Nex, F.; Kerle, N.; Vosselman, G. SATELLITE IMAGE CLASSIFICATION OF BUILDING
 215 DAMAGES USING AIRBORNE AND SATELLITE IMAGE SAMPLES IN A DEEP LEARNING
 216 APPROACH. *ISPRS Annals of Photogrammetry, Remote Sensing & Spatial Information Sciences* **2018**, *4*.
- 217 12. Huang, B.; Zhao, B.; Song, Y. Urban land-use mapping using a deep convolutional neural network with
 218 high spatial resolution multispectral remote sensing imagery. *Remote Sensing of Environment* **2018**, *214*, 73-
 219 86.
- 220 13. Huang, F.; Yu, Y.; Feng, T. Automatic building change image quality assessment in high resolution remote
 221 sensing based on deep learning. *Journal of Visual Communication and Image Representation* **2019**, *63*, 102585.
- 222 14. Bai, Y.; Mas, E.; Koshimura, S. Towards operational satellite-based damage-mapping using u-net
 223 convolutional network: A case study of 2011 tohoku earthquake-tsunami. *Remote Sensing* **2018**, *10*, 1626.
- 224 15. Cao, Q.D.; Choe, Y. Building damage annotation on post-hurricane satellite imagery based on
 225 convolutional neural networks. *Natural Hazards* **2020**, *103*, 3357-3376.
- 226 16. Wang, X.; Li, P. Extraction of earthquake-induced collapsed buildings using very high-resolution imagery
 227 and airborne lidar data. *International journal of remote sensing* **2015**, *36*, 2163-2183.
- 228 17. Cao, K.; Zhang, X. An Improved Res-UNet Model for Tree Species Classification Using Airborne High-
 229 Resolution Images. *Remote Sensing* **2020**, *12*, 1128.
- 230 18. Ji, M.; Liu, L.; Buchroithner, M. Identifying collapsed buildings using post-earthquake satellite imagery
 231 and convolutional neural networks: A case study of the 2010 Haiti earthquake. *Remote Sensing* **2018**, *10*,
 232 1689
- 233 19. UNITAR/UNOSAT; EC Joint Research Centre; World Bank. Haiti Earthquake 2010: Remote Sensing
 234 Damage Assessment. Available online: <https://unitar.org/maps/countries/44?page=0> (accessed on 17
 235 August 2019).
- 236 20. Berman, L. Haiti Earthquake Data (VECTORS). V1 ed.; Harvard Dataverse: 2015;
 237 doi:10.7910/DVN/BAGUVN.
- 238 21. Liu, D.; Han, L.; Han, X. High spatial resolution remote sensing image classification based on deep learning.
 239 *Acta optica sinica* **2016**, *36*, 0428001.
- 240 22. Sameen, M.I.; Pradhan, B.; Aziz, O.S. Classification of very high resolution aerial photos using spectral-
 241 spatial convolutional neural networks. *Journal of Sensors* **2018**, *2018*.
- 242 23. Wozniak, M. *Hybrid classifiers: methods of data, knowledge, and classifier combination*; Springer: 2013; Vol. 519.
- 243 24. Kemker, R.; Salvaggio, C.; Kanan, C. Algorithms for semantic segmentation of multispectral remote sensing
 244 imagery using deep learning. *ISPRS journal of photogrammetry and remote sensing* **2018**, *145*, 60-77.
- 245 25. Han, Y.; Wei, C.; Zhou, R.; Hong, Z.; Zhang, Y.; Yang, S. Combining 3D-CNN and Squeeze-and-Excitation
 246 Networks for Remote Sensing Sea Ice Image Classification. *Mathematical Problems in Engineering* **2020**, *2020*.
- 247 26. Ferreira, A.; Giraldo, G. Convolutional Neural Network approaches to granite tiles classification. *Expert*
 248 *Systems with Applications* **2017**, *84*, 1-11.
- 249 27. Garg, L.; Shukla, P.; Singh, S.K.; Bajpai, V.; Yadav, U. Land Use Land Cover Classification from Satellite
 250 Imagery using mUnet: A Modified Unet Architecture. In Proceedings of VISIGRAPP (4: VISAPP); pp. 359-
 251 365.
- 252 28. Chen, G.; Li, C.; Wei, W.; Jing, W.; Woźniak, M.; Blažauskas, T.; Damaševičius, R. Fully convolutional
 253 neural network with augmented atrous spatial pyramid pool and fully connected fusion path for high
 254 resolution remote sensing image segmentation. *Applied Sciences* **2019**, *9*, 1816
- 255 29. Li, E.; Xia, J.; Du, P.; Lin, C.; Samat, A. Integrating multilayer features of convolutional neural networks for
 256 remote sensing scene classification. *IEEE Transactions on Geoscience and Remote Sensing* **2017**, *55*, 5653-5665.

30. Han, J.; Zhang, D.; Cheng, G.; Guo, L.; Ren, J. Object detection in optical remote sensing images based on weakly supervised learning and high-level feature learning. *IEEE Transactions on Geoscience and Remote Sensing* **2014**, *53*, 3325-3337.
31. Ronneberger, O.; Fischer, P.; Brox, T. U-net: Convolutional networks for biomedical image segmentation. In Proceedings of International Conference on Medical image computing and computer-assisted intervention; pp. 234-241.
32. Zhang, Z.; Liu, Q.; Wang, Y. Road extraction by deep residual u-net. *IEEE Geoscience and Remote Sensing Letters* **2018**, *15*, 749-753.
33. Ural, S.; Hussain, E.; Kim, K.; Fu, C.-S.; Shan, J. Building extraction and rubble mapping for city port-au-prince post-2010 earthquake with GeoEye-1 imagery and lidar data. *Photogrammetric Engineering & Remote Sensing* **2011**, *77*, 1011-1023.
34. Leichte, T.; Geiß, C.; Lakes, T.; Taubenböck, H. Class imbalance in unsupervised change detection—a diagnostic analysis from urban remote sensing. *International journal of applied earth observation and geoinformation* **2017**, *60*, 83-98.
35. Ioffe, S.; Szegedy, C. Batch normalization: Accelerating deep network training by reducing internal covariate shift. *arXiv preprint arXiv:1502.03167* **2015**.
36. Haut, J.M.; Fernandez-Beltran, R.; Paoletti, M.E.; Plaza, J.; Plaza, A.; Pla, F. A new deep generative network for unsupervised remote sensing single-image super-resolution. *IEEE Transactions on Geoscience and Remote Sensing* **2018**, *56*, 6792-6810.
37. Springenberg, J.T.; Dosovitskiy, A.; Brox, T.; Riedmiller, M. Striving for simplicity: The all convolutional net. *arXiv preprint arXiv:1412.6806* **2014**.
38. Maggiori, E.; Tarabalka, Y.; Charpiat, G.; Alliez, P. Can semantic labeling methods generalize to any city? the inria aerial image labeling benchmark. In Proceedings of 2017 IEEE International Geoscience and Remote Sensing Symposium (IGARSS); pp. 3226-3229.
39. Deep Learning Studio, AI services on Deep Cognition. Available online: <https://deepcognition.ai/features/deep-learning-studio/> (accessed on 27 September 2020).
40. Artificial intelligence software on Peltarion. Available online: <https://peltarion.com/> (accessed on 27 September 2020).
41. Bai, Y.; Adriano, B.; Mas, E.; Koshimura, S. Building damage assessment in the 2015 Gorkha, Nepal, earthquake using only post-event dual polarization synthetic aperture radar imagery. *Earthquake Spectra* **2017**, *33*, 185-195.
42. Bai, Y.; Gao, C.; Singh, S.; Koch, M.; Adriano, B.; Mas, E.; Koshimura, S. A framework of rapid regional tsunami damage recognition from post-event TerraSAR-X imagery using deep neural networks. *IEEE Geoscience and Remote Sensing Letters* **2017**, *15*, 43-47.



© 2020 by the authors; licensee MDPI, Basel, Switzerland. This article is an open access article distributed under the terms and conditions of the Creative Commons by Attribution (CC-BY) license (<http://creativecommons.org/licenses/by/4.0/>).